Proceedings Paper:
Hayajneh, AM, Zaidi, SAR, McLernon, DC orcid.org/0000-0002-5163-1975 et al. (1 more author) (2017) Performance Analysis of UAV Enabled Disaster Recovery Network: A Stochastic Geometric Framework based on Matern Cluster Processes. In: IET 3rd International Conference on Intelligent Signal Processing (ISP 2017). ISP 2017, 04-05 Dec 2017, London, UK. Institution of Engineering and Technology . ISBN 978-1-78561-707-2

https://doi.org/10.1049/cp.2017.0347

Performance Analysis of UAV Enabled Disaster Recovery Network: A Stochastic Geometric Framework based on Matern Cluster Processes

Ali Mohammad Hayajneh, Syed Ali Raza Zaidi, Des C. McLernon and Mounir Ghogho

***Abstract*—Drones will be employed by Facebook and Google for capacity off-loading in front/back hauling scenarios utilizing drone-empowered autonomous heterogeneous networks. But in another application, drone-based, post-disaster recovery of communication networks will also be of crucial importance in the design of future smart cities. So, in order to address the design issues of these latter networks, we present (from a stochastic geometric perspective) a comprehensive statistical framework for the spatial distribution of these hybrid user-centric drone/micro cellular networks. We introduce the novel idea of using a Stenien's cell (with variable radius) to model the region over which the drones will be distributed and the drones will effectively form a Matern cluster process (MCP) across the original network space. We then employ this newly developed framework to investigate the impact of changing several parameters on the performance of the new drone small-cell clustered networks (DSCCNs) and we develop appropriate closed-form expressions that model the performance (later validated via Monte Carlo simulations).**

***Index Terms*—Drone, Public safety, Stochastic geometry, Unmanned aerial vehicles, Coverage probability, Optimization, Heterogeneous networks.**

I. Introduction

Drones, also called unmanned aerial vehicles (UAVs), will have an important role to play in future communication networks that includes public safety, capacity off-loading and post-disaster recovery (to name but a few applications) [1]–[4].

A. Motivation and Related Work

Recently, public safety networking has received significant attention within the third generation partnership project (3GPP) standardization. 3GPP is currently in the process of standardizing proximity services (ProSe) via Device-to-Device (D2D) communication. The central idea behind ProSe is to form an ad-hoc network where certain nodes of the network may still have access to operational cellular infrastructure in a post-disaster situation.

Despite the growing popularity of the aforementioned, drone assisted networks present an attractive alternative and complementary deployment option. That is, drones can offer many advantages to typical ad-hoc networks: (i) they presents fast and resilient deployment; (ii) they can be controlled via a centralized network operator to increase compatibility and interoperability, and (iii) the propagation conditions are much more favorable and can be further optimized by exploiting controlled mobility of the drones. Here, we will focus on building an analytical statistical framework to study the randomness of the network by harnessing stochastic geometry tools in a user-centric fashion in contrast to previous works [5]–[9].

This work is partially funded by The Hashemite University (HU), Zarqa, Jordan.

A. M. Hayajneh, S. A. R. Zaidi, Des. C. McLernon and M. Ghogho are with the School of Electronic and Electrical Engineering, University of Leeds, Leeds LS2 9JT, United Kingdom, e-mail: elamh,s.a.zaidi,d.c.mclernon,m.ghogho@leeds.ac.uk. M. Ghogho is also affiliated with the International University of Rabat, Morocco.

In our previous work in [6], we studied the coverage probability for a constrained recovery area where the destruction is assumed to be in a small circular region of the space. However, this is not the case for the performance of the whole network space recovery. So we introduce the clustered-based recovery network structure to show a whole network open space scenario.

In order to define the framework for studying such networks, we will focus on cluster-based analytics and Stienen's model as an enhancement. Due to the implicit complexity of heterogeneous communication networks, there is an emerging research area employing and developing a more realistic framework for the study of the network. User-centric network distributions are widely adopted in the modeling of current heterogeneous networks [10], [11]. But the uniform homogeneous Poisson point process (HPPP) that is used does not faithfully represent the cellular network structure. Hence, cluster-based analytics that correlate the user and base stations locations have a better representation and more accurate performance analysis. In particular, the Matern's cluster process (MCP), as an example of the Neman-Scott cluster processes, are widely used for the representation of cluster-based distributions of mobile users and base stations (BS). However, clustering in the previous works comes from the physical distribution of the users. But in our proposed network structure, clustering will come from the recovery drone base stations (DBSs) distributions which is correlated to the holes representing the centers of the clusters constructed by the flying DBSs.

In addition to the correlation between the users and base station locations, in post-disaster scenarios we need more than one flying drone small cell (DSC) to off-load the same capacity that has been carried by the destroyed traditional base stations [6]. As a result, the distribution of these drones around the center of the destruction area and inside of the hole will form a cluster-based process, where the drones are acting as a daughter points of a cluster process and the parent points are the points from the traditional network due to the uniform thinning (i.e., destruction of base stations). With this re-configuration of the network, we simply build a drone-based back/front-hauling network. However, the radius of the recovery in every hole is not fixed and needs to be defined. This is a result of the variable Voronoi cell size which in fact has a Rayleigh distribution and is called a Stienen's cell radius [12], [13]. So, unlike other papers where the radius of the cluster is fixed, we will use a variable cluster radius defined by the Stienen's model.

B. Contribution & Organization

The contribution and organization of this paper are as follows:

1) The comprehensive spatial modeling of a drone-based user-centric clustered public safety network is considered over a partially destructed/off-loaded cellular network. The impact of various parameters such as path-loss, number of DBSs, density of micro base stations

(MBSs) and the altitude of the DBSs on both the DSCN and the cellular network coverage is investigated (see section II).
2) Borrowing tools from stochastic geometry, we present a statistical framework for quantifying the performance of large scale DSCNs deployment for different scenarios of the implementation geometry. Also, the analytical framework is subsequently employed for design optimization by studying the effect of changing some of the design parameters.
3) The impact of the number of DBSs (and their height) on the coverage probability performance metric for drone mobile users (DMUs) is investigated (see section IV).
4) Finally, some critical design issues (explored for future developments) are also summarized (see section VII).

C. Notation.

Throughout this paper, we employ the following mathematical notations. The counting measure of a point process $\Phi(\mathcal{B})$ provides a count of points inside the compact closed subset $\mathcal{B} \in \mathbb{R}^2$ (i.e., bounded area). The probability density function (PDF) for a random variable X is represented as $f_X(x)$ with the cumulative density function written as $F_X(x)$. The exclusion symbol $\setminus$ represents the exclusion of a subset from a superset. The expectation of a function $g(X)$ of a random variable X is represented as $\mathbb{E}_X[g(X)]$. The bold-face lower case letters (e.g., $\mathbf{x}$) are employed to denote a vector in $\mathbb{R}^2$ and $\|\mathbf{x}\|$ is its Euclidean norm. The Laplace transform (LT) of any random variable Z is $\mathcal{L}_Z(s)$ (i.e., LT of the PDF of the random variable).

II. Network and Propagation model

A. Deployment Geometry

Spatial Model for Post-disaster Cellular Network: Consider a large scale macro-cellular network where the locations of the BSs is modeled by a HPPP $\Phi = \{\mathbf{x_0}, \mathbf{x_1}, ..., \mathbf{x}_\infty, \forall\ \mathbf{x}_i \in \mathbb{R}^2\}$ (as in [14]) with density λ. The post-disaster cellular network is constructed by location independent thinning of Φ with probability of thinning p^o. More specifically:

$$\Phi_\mu = \{\mathbf{x} \in \Phi : \mathbb{1}(\mathbf{x}) = 1\} \text{ with density } \lambda_\mu = p_s\lambda, \quad (1)$$

where $\mathbb{1}(.)$ denotes a Bernoulli random variable. Notice that the thinning process results in a new HPPP Φ_μ which has density λ_μ such that $\lambda_\mu = (1-p^o)\lambda = p_s\lambda$, where p_s is the BS survival probability. So, a new HPPP Φ_S will result from the thinning and the translation such that

$$\Phi_S = \Phi \setminus \Phi_\mu, \quad (2)$$

which has a density $\lambda_S = p^o\lambda$.

Network Model for DSCN: In order to fill the coverage holes N_d DSCs are deployed as replacements for each destructed BS in Φ_s. As Φ_s in the HPPP, such deployment topology results in a Poisson cluster process. Then the union of all the DSCs in the space around the parent Poisson process Φ_S with intensity λ_S forms a cluster process defined as

$$\Phi_C \triangleq \bigcup_{i\in\{0,2,...,n-1\}} \{\Phi_{C_i} + \mathbf{x}_i\}, \quad (3)$$

where Φ_{C_i} is a cluster with N_d DCSs such that $\Phi_{C_i} = \{\mathbf{y_1}, ..., \mathbf{y}_{N_d}, \forall\ \mathbf{y}_i \in \mathbb{R}^2\}$ and n is the number of elements in Φ_S. Also, the clusters in Φ_C, without loss of generality, are divided into two sets of clusters: (i) the one called the representative cluster which contains the set of all points around $\mathbf{x_0}$ and is defined by $\Phi_{C_{in}} \triangleq \Phi_{C_0}$, and (ii) the set of all cluster process points except the points in the representative cluster and is defined by $\Phi_{C_{out}} \triangleq \Phi_C \setminus \Phi_{C_0}$[1].

We assume that the DSCs are uniformly distributed around each destroyed MBS thus forming the well known Matern's cluster process (MCP). In a MCP, a fixed number of points (N_d) are distributed uniformly in the two dimensional space according to the density function

$$f^M(\mathbf{x}) = \frac{1}{\pi\sigma_M^2}, \|\mathbf{x}\| \le \sigma_M, \quad (4)$$

where σ_M is the radius of the cluster. Then the distribution of the points around the cluster center follows the PDF $f_R^M(r) = \frac{2r}{\sigma_M^2}$. We introduce a modified Matern's model where the radius of the cluster is actually dependent upon the size of the Stienen cell of the destroyed MBS. This is considered a good approximation for the radius of the destroyed cell. We also modify the traditional models of a Poisson cluster processes to integrate the implicit size changing cells effect for a more realistic recovery model. Thus, the distribution of σ_M is considered to be the same distribution as the generalized Stienen's cell radius, i.e.,

$$f_{\sigma_M}(\sigma_M) = 2\pi\lambda\tau\sigma_M \exp\left(-\pi\lambda\tau^2\sigma_M^2\right). \quad (5)$$

Here, setting the value of $\tau = 2$ gives the distribution of the radius of the maximum inscribed circle centered on the position of the destroyed MBS and equal to half of the distance to the nearest neighbor in the original tessellation which is the well-known Stienen's cell radius. Tunning the value of τ will tune the radius of the recovery area where the DBSs will be distributed.

Spatial Model for MUs: It is assumed that the distribution of the users around the center of the clusters is the same as the DBSs with the same density. This follows from the fact that every DBS is associated to only one user in the same channel resource block. Hence, we map $\Phi_C \mapsto \Phi_C^u$ for the set of the users around cluster centers with density $\lambda_C \mapsto N_d\lambda_C^u$.

B. Propagation Model

Path Loss Model: Combining the LoS/NLoS losses and LoS/NLoS probability as in [2], the total average path-loss from MU to DBS can be quantified as:

$$\bar{l}_d(r) = \bar{\kappa}^{-1}(r)(r^2+h^2)^{-1}, \quad (6)$$

where $\bar{\kappa}(r) = K_{NLoS} + \frac{K_{LoS}-K_{NLoS}}{1+a_1\,\mathrm{e}^{-b_1\eta\,\tan^{-1}(\frac{h}{r})+b_1\,a_1}}$, K_{LoS} and K_{NLoS} are environment and frequency dependent parameters such that $K_i = \zeta_i\left(c/(4\pi f_{MHz})\right)^{-\alpha}$, ζ_i is the excess path loss for $i \in \{LoS, NLoS\}$ and α is the path loss exponent which is equal to 2 (as can be found in the literature of drone-based small cell applications), a_1, b_1, c_1 are environment dependent constants, $\eta = 180/\pi$ and h is the drone altitude. The large scale path loss for the down-link of the cellular network is modeled by the well-known power law path loss function

$$l_\mu(r) = K^{-1}r^{-\alpha}, \quad (7)$$

where α (the path loss exponent) has typical values for small/micro cells between 2 and 4. K is the excess path loss

[1]We also write $\Phi_{C_\mathbf{x}} = \Phi_{C_i}$ to denote to the cluster around the parent point $\mathbf{x}_i \in \Phi_S$.

coefficient and has typical values between 100 dB and 150 dB (see [15] for details).

Small Scale Fading: It is assumed that large scale path loss is complemented with small scale Rayleigh fading such that $|g|^2 \sim \text{Exp}(1)$. Also, it is assumed that the network is operating in an interference limited regime, i.e., the performance of all links is dependent upon co-channel interference and the thermal noise at the receiver front-end is negligible.

C. Transmission Model

In this paper we assume that the DMU is associated to nearest BS (i.e., the BS which maximizes average received SNR) and transmitters on the same frequency are considered as co-channel interferers. These out-of-cell interferers can be classified into three categories: (i) the interference received from MBSs working on the same channel as the serving DBS, (ii) the interference from the set of DBSs located inside the representative cluster and called "intra-cluster interferers", and (iii) the interferers from out of the representative cluster and called "inter-cluster interferers".

Lastly, we assume that the average number ($\bar{N}_d$) of co-channel active DBSs inside any of the clusters has a Poisson distribution which is also related to the number of channel resources used (N_c) by $\bar{N}_d = \frac{N_d}{N_c}$.

III. Distance Distributions for MCP

In this section, we characterize link distance distributions which are required to quantify the large scale path-loss given by (6). These distributions are employed to quantify coverage probability in section IV. We consider a typical user at location $\|\mathbf{x}\| = V_o$ from the center of the representative cluster and served by the link to the nearest DBS with a distance $R_1 = \|\mathbf{x} - \mathbf{y_1}\|$ where $\mathbf{y_1}$ represents the location of the nearest DBS. Then to evaluate the distribution of the distance R_1, we need to make a random variable transformation and then apply order statistics rules on the well-known distribution of the DBSs distance R to cluster center which has the PDF:

$$f_R^M(r) = \frac{2r}{\sigma_M^2},\ 0 \le r \le \sigma_M, \tag{8}$$

and CDF $F_R^M(r) = \frac{r^2}{\sigma_M^2},\ 0 \le r \le \sigma_M$[2]. Then, by performing a joint random variable transformation of $f_R^M(r)$ such that $D(r, v_o) = \sqrt{v_o^2 + r^2 - 2v_o r\cos(\theta)}$ where θ is the angle between the lines R and V_o with the PDF $f_\Theta(\theta) = \frac{1}{2\pi}, 0 \le \theta \le 2\pi$, the distribution of the distance D will have the PDF (9) and the CDF can be easily obtained by integrating the PDF [16][3].

Next, the distribution of the distance $R_1 = r_1$ from the typical MU and the nearest DBS can be evaluated as in the next proposition.

Proposition 1. *The PDF of the distance $R_1 = r_1$ from the typical user at a distance V_o from the cluster center to the nearest DBSs for MCP can be evaluated as in* (10) *on the next page.*

Proof. Let N_d BSs be distributed uniformly inside a circle of radius σ_M, Then the derivation of the nearest neighbor distribution amongst the N_d DBSs follows the order statistics using the fact that for general N_d i.i.d random variables $Z_i \in \{Z_1, Z_2, ..., Z_{N_d}\}$ with PDFs $f_{Z_i}(z)$ ordered in ascending order. Then the PDF of $Z_1 = \min_i(Z_i)$ can be written as $f_{Z_1}(z) = N\left(1 - F_{Z_i}(z)\right)^{N-1} f_{Z_i}(z)$ [17]. Then, by applying this to (9), we can write the density of the distance R_1 as

$$f_{R_1}^M(r_1|v_o, \sigma_M) = \begin{cases} f_{R_1^{(1)}}^M(r_1|v_o, \sigma_M), & 0 \le r_1 \le \sigma_M - v_o, \\ f_{R_1^{(2)}}^M(r_1|v_o, \sigma_M), & \sigma_M - v_o < r_1 \le \sigma_M + v_o \end{cases} \tag{11}$$

where

$$f_{R_1^{(1)}}^M(r_1|v_o, \sigma_M) = N_d(1 - F_{R^{(1)}}^M(r_1|v_o, \sigma_M))^{N_d - 1} f_{R^{(1)}}^M(r_1|v_o, \sigma_M) \tag{12}$$

$$f_{R_1^{(2)}}^M(r_1|v_o, \sigma_M) = N_d(1 - F_{R^{(2)}}^M(r|v_o, \sigma_M))^{N_d - 1} f_{R^{(2)}}^M(r_1|v_o, \sigma_M). \tag{13}$$

■

Proposition 2. *The distribution of distance $R_x = r_x$ from the in-cluster DBSs interferers to the typical user located at distance V_o from the cluster center (conditioned that the nearest neighbor DBS is at distance $R_1 = r_1$ with the distribution in* (10)*) can be written as*

$$f_{R_x}^M(r_x|v_o, r_1) = \begin{cases} \frac{2r_x}{\sigma_M^2 - r_1^2}, & 0 \le r_x \le \sigma_M - v_o, \\ \frac{\frac{2r_x}{\pi\sigma_M^2}\arccos\left(\frac{r_x^2 + v_o^2 - \sigma_M^2}{2v_o r_x}\right)}{1 - \psi}, & \sigma_M - v_o < r_x \le \sigma_M + v_o. \end{cases} \tag{14}$$

Proof. The proof of this is simple. Following from the fact that the distance to the nearest interferer is larger than the serving distance R_1, then the area of circle formed by the distance from the typical user and the serving DBS is truncated from the whole area. Therefore, we can write the conditional distribution of this event as follows:

$$f_{R_x}^M(r_x|v_o, \sigma_M, r_1) = f_R^M(r_x|v_o, \sigma_M), R > R_1 = r_1 = \frac{f_R^M(r_x|v_o, \sigma_M)}{1 - F_R^M(r_1|v_o, \sigma_M)}. \tag{15}$$

Hence, by substituting $f_R^M(r_x|v_o, \sigma_M)$ and its CDF, we complete the proof of (14). ■

Following from the above proposition, we can easily show that the distribution of distances from the typical user at V_o to the out-of-cluster interferers can be evaluated in the next proposition.

Proposition 3. *The PDF of the distance distribution from the typical user at distance V_o from the cluster center to the interfering DBSs from out of the representative cluster can be written as*

$$f_{R_o}^M(r_o|u, \sigma_M) = f_R^M(r_o|u, \sigma_M). \tag{16}$$

Proof. The proof of this follows the same steps as for (9) by doing the joint transformation for the uniformly chosen DBS. ■

[2]We also assume that the distance $V_o = v_o$ from the DMU to the cluster center is a random variable with the PDF $f_{V_o}^M(v_o) = \frac{2v_o}{\sigma_M^2},\ 0 \le v_o \le \sigma_M$.

[3]We use $f_R^M(r|v_o)$ to represent the PDF of D with slight notation abuse.

$$f_R^M(r|v_o,\sigma_M)=\begin{cases} f_{R^{(1)}}^M(r|v_o,\sigma_M)=\frac{2r}{\sigma_M^2}, & 0\le r\le \sigma_M-v_o,\\ f_{R^{(2)}}^M(r|v_o,\sigma_M)=\frac{2r}{\pi\sigma_M^2}\arccos\left(\frac{r^2+v_o^2-\sigma_M^2}{2v_o r}\right), & \sigma_M-v_o<r\le\sigma_M+v_o. \end{cases} \tag{9}$$

$$f_{R_1}^M(r_1|v_o,\sigma_M)=\begin{cases} f_{R_1^{(1)}}^M(r_1|v_o,\sigma_M)=\frac{2N_d r_1}{\sigma_M^2}\left(1-\frac{r_1^2}{\sigma_M^2}\right)^{N_d-1}, & 0\le r_1\le \sigma_M-v_o,\\ f_{R_1^{(2)}}^M(r_1|v_o,\sigma_M)=\frac{2N_d r_1}{\pi\sigma_M^2}\arccos\left(\frac{r_1^2+v_o^2-\sigma_M^2}{2v_o r_1}\right)(1-\psi)^{N_d-1}, & \sigma_M-v_o<r_1\le\sigma_M+v_o. \end{cases} \tag{10}$$

where $\psi=\frac{r_1^2}{\pi\,\sigma_M^2}\left(\theta_1^1-\frac{1}{2}\sin\left(2\,\theta_1^1\right)\right)+\frac{1}{\pi}\left(\theta_2^1-\frac{1}{2}\sin\left(2\,\theta_2^1\right)\right)$, $\theta_1^1=\arccos\left(\frac{{r_1}^2-\sigma_M^2+v_o}{2v_o r_1}\right)$ and $\theta_2^1=\arccos\left(\frac{-{r_1}^2+\sigma_M^2+v_o}{2v_o\sigma_M}\right)$.

IV. Coverage Probability

In order to characterize the link level performance of DSCNs, we employ coverage probability as a metric. The coverage probability of an arbitrary user is defined as the probability at which the received signal to interference ratio (SIR^{M_s}) is larger than a pre-defined threshold, β such that

$$P_c^{M_s}=\Pr\{\text{SIR}^{M_s}\ge\beta\}. \tag{17}$$

Then, considering that both the DBSs and the MBSs networks are sharing the same channel resources, SIR^{M_s} can be quantified as,

$$\text{SIR}^{M_s}=\frac{P_d\,|g|^2\,\bar{l}_d(r_1)}{I_{\Phi_{C_{in}}}+I_{\Phi_{C_{out}}}+I_{\Phi_\mu}}=\frac{P_d\,|g|^2\,\bar{l}_d(r_1)}{I_{tot}}. \tag{18}$$

where

$$I_{\Phi_{C_{in}}}=\sum_{\mathbf{y}\in\Phi_{C_{in}}}P_d\,|g|^2\,\frac{\left(h^2+\|\mathbf{x_0}+\mathbf{y}\|^2\right)^{-1}}{\bar{\kappa}\left(\|\mathbf{x_0}+\mathbf{y}\|\right)}$$

$$I_{\Phi_{C_{out}}}=\sum_{\mathbf{x}\in\Phi_S\setminus\mathbf{x_0}}\sum_{\mathbf{y}\in\Phi_{C_\mathbf{x}}}P_d\,|g|^2\,\frac{\left(h^2+\|\mathbf{x}+\mathbf{y}\|^2\right)^{-1}}{\bar{\kappa}\left(\|\mathbf{x}+\mathbf{y}\|\right)}$$

$$I_{\Phi_\mu}=\sum_{\mathbf{x}\in\mathbf{\Phi}_\mu}P_\mu\,|g|^2\,l_\mu(\|\mathbf{x}\|). \tag{19}$$

Here r_1 represents the distance from the DMU to the nearest DBS; $|g|^2$ is the channel power gain coefficient and it is assumed to be the same for all the links; $I_{\Phi_{C_{in}}}$ represents the received interference from the DBSs in the representative cluster; $I_{\Phi_{C_{out}}}$ represents the received interference from the co-channel DBSs concurrently transmitting with the considered representative link from out of the cluster; I_{Φ_μ} is the interference received from the retained MBSs; and P_μ and P_d are the transmit power for the MBS and DBS respectively.

In light of the above, the coverage probability can be evaluated as

$$\begin{aligned} P_c^{M_s} &= \Pr\{\text{SIR}^{M_s}\ge\beta\}\overset{(a)}{=}\mathbb{E}_{r_1}[\mathbb{E}_{I_{tot}}[\exp\left(-sI_{tot}\right)]],\\ &\overset{(b)}{=}\mathbb{E}_{r_1}[\mathcal{L}_{I_{\Phi_{C_{out}}}}(s|r_1,\sigma_M)\mathcal{L}_{I_{\Phi_{C_{in}}}}(s|r_1,\sigma_M)\mathcal{L}_{I_{\Phi_\mu}}(s)], \end{aligned} \tag{20}$$

where $s=\beta\left(r_1^2+h^2\right)\bar{\kappa}(r_1)/P_d$, (a) is obtained by averaging over the channel coefficient and (b) is obtained by applying the definition of the Laplace transform and then using the addition property of the Laplace transformation of independent random variables.

A. Coverage Probability for MCP

To complete the analysis of the coverage probability, we need to quantify the Laplace transformations for the interference at the typical DMU. In the next lemma, we introduce the Laplace transform of the distribution of the in-cluster interference for the MCP.

Lemma 1. *The Laplace transform of the interference at the DMU from the in-cluster DBSs for MCP can be evaluated as*

$$\mathcal{L}_{I_{\Phi_{C_{in}}}}(s)=\sum_{i=1}^{N_d}\left(\int_{r_1}^{\infty}\frac{f_{R_x}^M(r_x|v_o,\sigma_M)}{1+\frac{sP_d}{\bar{\kappa}(r_x)(h^2+r_x^2)}}\,\mathrm{d}r_x\right)^{i-1}\xi(i,N_d), \tag{21}$$

where $\xi(i,N_d)=\bar{N}_d^i\exp(-\bar{N}_d)/i!\Sigma_{k=1}^{N_d}\frac{\bar{N}_d^k\exp(-\bar{N}_d)}{k!}$.

Proof. Please refer to Appendix A. ∎

In order to complete the analysis of the coverage probability, we also need to derive the Laplace transform of the interference from out-of-cluster DBSs - see Lemma 2.

Lemma 2. *The Laplace transform of the interference distribution at the DMU from out-of-cluster DBSs for MCP can be evaluated as in* (22)*.*

Proof. Please refer to Appendix B. ∎

Now, we will relax the dependency between the drone network parent points and the location of the retained base stations to evaluate the Laplace transform of the interference at the DMU from the surviving MBSs.

Lemma 3. *The Laplace transform of the interference distribution (at the drone typical user) from the retained MBSs with density $\lambda_\mu=(1-p^o)\lambda$ can be approximated as follows:*

$$\mathcal{L}_{I_{\Phi_\mu}}(s)=\mathbb{E}(\exp(-sI_{\Phi_\mu}))\overset{(a)}{=}\exp\Big(-2\pi\frac{\lambda_\mu}{N_c}\frac{s^{-\frac{2}{\alpha}}P_\mu^{-\frac{2}{\alpha}}}{K^{-\frac{2}{\alpha}}\text{sinc}\left(\frac{2}{\alpha}\right)}\Big). \tag{23}$$

Proof. The proof of this is straightforward from the Laplace transform of the PPP where (a) is obtained by taking the expectation over the fading channel coefficient assuming i.i.d Rayleigh channels followed by the probability generating functional (PGFL) of the PPP then followed by Cartesian to polar transformation. ∎

In the next theorem, we evaluate the coverage probability for a drone typical user with fixed recovery cell radius.

$$\mathcal{L}_{I_{\Phi_{C_{out}}}}(s) = \exp\Big(-2\pi\lambda_S \int_0^{\infty}\Big(1-\exp\Big(-\frac{N_d}{N_c}\int_0^{\infty}\Big(1-\frac{1}{1+sP_d\bar{\kappa}(r_o)(h^2+r_o^2)}\Big)f_{R_o}^{M}(r_o|u,\sigma_M)\,\mathrm{d}r_o\Big)\Big)u\,\mathrm{d}u\Big). \quad (22)$$

TABLE I: Simulation parameters.

Parameter	Value	Description
$\zeta_{LoS}, \zeta_{NLoS}$	1,20 dB	Excess path loss
f_{MHz}	900 MHz	Carrier frequency
α	3.5	Path loss exponent
K	132 dB	Excess path loss for micro cells
a_1, b_1	9.6, 0.28	Environment dependent constants
λ_1	1×10^{-5}	Base stations density
N_c	3, 2	Available number of channels
P_d	2 dBW	Drone cell transmission power
P_μ	5 dBW	MBS cell transmission power

Theorem 4. *The coverage probability of drone typical user with fixed recovery cell radius σ_M can be evaluated for Matern's cluster processes as*

$$P_c^{M_s} = \int_0^{\infty}\int_0^{\infty}\int_0^{\infty}\mathcal{L}_{I_{\Phi_{C_{out}}}}(s)\mathcal{L}_{I_{\Phi_{C_{in}}}}(s)\mathcal{L}_{I_{\Phi_{\mu}}}(s) \times f_{R_1}^{M}(r_1|v_o,\sigma_M)f_{V_o}^{M}(v_o)f_{\sigma_M}(\sigma_M)\,\mathrm{d}r_1\,\mathrm{d}v_o\,\mathrm{d}\sigma_M. \quad (24)$$

V. Area Spectral Efficiency and Energy Efficiency

Until now, we have studied the coverage probability as a link level performance analysis. To cover the whole network figures of performance, we need to study the Area Spectral Efficiency (ASE) of the network in order to perform a network level performance analysis. In this section we show analysis of ASE for MCP.

Proposition 4. *Given the coverage probability in* (24)*, the throughput (i.e., Area Spectral Efficiency) of the network for the modified MCP can be evaluated as*

$$\mathcal{T}_M = ASE_M = \lambda_C N_d N_c P_c^{M_s}\log_2(1+\beta). \quad (25)$$

For a comprehensive study of the network, we also make use of the term energy efficiency (E_{eff}). The E_{eff} in general can be evaluated as [18]:

$$E_{eff} = \frac{\text{Area Spectral Efficiency}}{\text{Average Network Power Consumption}} = \frac{\mathcal{T}_M}{\lambda_C N_d P_d}, \quad (26)$$

$$= \frac{N_c P_c^{M_s}\log_2(1+\beta)}{P_d}\ \text{b/J/Hz}. \quad (27)$$

With the above expressions for the coverage probability and energy efficiency, then we can study the performance of the UAV assisted recovery networks. In the the next section, we will show the results and present discussion of the proposed model.

VI. Results and Discussion

In this section, we show numerical results for the coverage probability ($P_c^{M_s}$) and the energy efficiency (E_{eff})of drone-based communication recovery network deployment. Furthermore, we assume that the DBCN is operating in an urban environment with the parameters shown in Table I. Also, as described in the previous sections, we consider a Rayleigh fading wireless channel. The discussion will consider both of these.

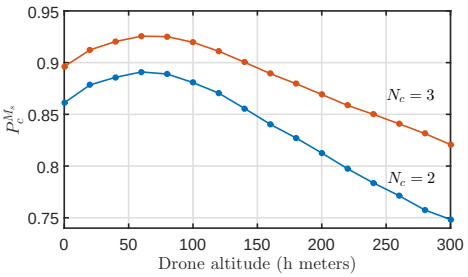

Fig. 1: Coverage probability for arbitrarily chosen DMU for Stenien's recovery for MCP (see (24)). Original MBS and MU densities is $\lambda = 1\times10^{-6}$. The destruction probability $p^o = 0.1$. $\alpha = 3.5$. $N_d = 5$ and $P_d/P_\mu = 0.2$.

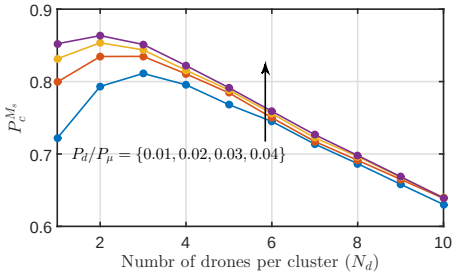

Fig. 2: Coverage probability for DMU. Original MBS and MU densities is $\lambda = 1\times10^{-6}$, the destruction probability $p^o = 0.1$. $\alpha = 3.5$ and $P_d/P_\mu = \{1,2,3,4\}\times10^{-2}$.

Figure 1 depicts the coverage probability against the altitude of the drones for a MCP where the Stenien's cell size is deployed (see (24)). The coverage probability shows that for a thinning probability of 0.1, where 5 drones are deployed in every cluster, there is an optimal drone altitude which is changing slightly alongside with the number of channels deployed. For example, there is an altitude difference of 20m when increasing the number of channels from 2 to 3. This also increases the coverage probability. Also, the change of coverage probability while changing the number of channels is not fixed and we notice that it is increasing while increasing the altitude of drones.

Figure 2 shows the coverage probability against the number of drones per cluster for multiple configuration of transmit power ratios for MCP where the Stenien's cell size is deployed (see (24)). The coverage probability curves show that, for a fixed transmit power ratio, there is an optimal number of drones at which the higher densification of the clusters will not increase the coverage probability. For example, for the configuration where the ratio $P_d/P_\mu = 1\%$, we need only 3 drones to achieve the optimal coverage. But, this cannot be said without looking at the energy efficiency metrics. That is, the densification of the of the network will increase the throughput while the coverage will only slightly change.

Figure 3 shows the energy efficiency against the number of drones per cluster for multiple configurations of the transmit power ratios for MCP where the Stenien's cell size is deployed (see (26)). No optimal number of drones can be seen for the energy efficiency. That is, as we increase the number of the

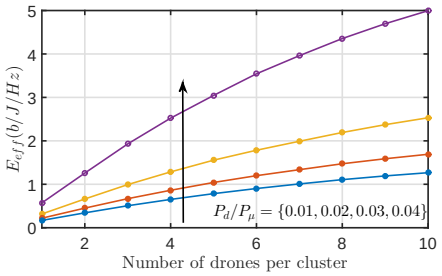

Fig. 3: Energy efficiency for drone mobile user. Original MBS is $\lambda = 1\times10^{-6}$, the destruction probability $p^o = 0.1$, $\alpha = 3.5$, and $P_d/P_\mu = \{1, 2, 3, 4\} \times 10^{-2}$.

drones we increase the network throughput. Moreover, the trend of the energy efficiency is to increase as we increase the transmit power ratio.

VII. Conclusion

In this paper, we introduced a statistical and analytical framework for evaluating the coverage probability and energy efficiency performance metrics for cluster based drones enabled recovery networks. Results show that there are a number of parameters which influence optimal deployment of the recovery network: (i) number of drones in a cluster, (ii) drone altitudes, (iii) transmission power ratio between drone base stations and traditional base station and (iv) the recovery area radius. Furthermore, it is also shown that by optimizing these parameters the coverage probability and the energy efficiency of a ground user can be significantly enhanced in a post-disaster situation.

Appendix A
Proof of Lemma 1

The Laplace transform of the interference from in-cluster DBSs at a typical DMU can be evaluated as

$$\mathcal{L}_{I_{\Phi_{C_{in}}}}(s) = \mathbb{E}\Big[\exp\Big(-s\sum_{\mathbf{y}\in\Phi_{C_{in}}} P_d\,|g|^2\,\frac{\left(h^2+\|\mathbf{x_0}+\mathbf{y}\|^2\right)^{-1}}{\bar{\kappa}\left(\|\mathbf{x_0}+\mathbf{y}\|\right)}\Big)\Big]$$
$$= \mathbb{E}\Big[\prod_{\mathbf{y}\in\Phi_{C_{in}}}\frac{1}{1+sP_d\frac{1}{\bar{\kappa}\left(\|\mathbf{x_0}+\mathbf{y}\|\right)\left(h^2+\|\mathbf{x_0}+\mathbf{y}\|^2\right)}}\Big]$$
$$= \sum_{i=1}^{N_d}\left(\int_0^\infty \frac{1}{1+\frac{sP_d}{\bar{\kappa}(\|\mathbf{x_0}+\mathbf{y}\|)(h^2+\|\mathbf{x_0}+\mathbf{y}\|^2)}} f^M(y)\,\mathrm{d}y\right)^{i-1}$$
$$\times \underbrace{\frac{\bar{N}_d^i\exp(-\bar{N}_d)}{i!\Sigma_{k=1}^{N_d}\frac{\bar{N}_d^k\exp(-\bar{N}_d)}{k!}}}_{\xi(i,N_d)}$$
$$= \sum_{i=1}^{N_d}\left(\int_0^\infty \frac{1}{1+\frac{sP_d}{\bar{\kappa}(r_x)(h^2+r_x^2)}} f_{R_x}^M(r_x|v_o,r_1)\,\mathrm{d}r_x\right)^{i-1}$$
$$\times\xi(i,N_d). \quad (28)$$

Appendix B
Proof of Lemma 2

The Laplace transform of the interference from out-of-cluster DBSs at a typical DMU can be evaluated as

$$\mathcal{L}_{I_{\Phi_{C_{out}}}}(s) =$$

$$\mathbb{E}\Big[\exp\Big(-s\sum_{\mathbf{x}\in\Phi_S\setminus\mathbf{x_0}}\sum_{\mathbf{y}\in\Phi_{C_\mathbf{x}}} P_dG\frac{\left(h^2+\|\mathbf{x}+\mathbf{y}\|^2\right)^{-1}}{\bar{\kappa}\left(\|\mathbf{x}+\mathbf{y}\|\right)}\Big)\Big]$$
$$= \mathbb{E}_{\Phi_S}\Big[\prod_{\mathbf{x}\in\Phi_S\setminus\mathbf{x_0}}\mathbb{E}_{\Phi_{C_\mathbf{x}}}\Big[\prod_{\mathbf{y}\in\Phi_{C_\mathbf{x}}}\frac{1}{1+sP_d\frac{\left(h^2+\|\mathbf{x}+\mathbf{y}\|^2\right)^{-1}}{\bar{\kappa}\left(\|\mathbf{x}+\mathbf{y}\|\right)}}\Big]\Big]$$
$$= \exp\Big(-2\pi\lambda_S\int_0^\infty\Big(1-\exp\Big(-\frac{N_d}{N_c}\int_0^\infty$$
$$\times\Big(1-\frac{1}{1+sP_d\frac{1}{\bar{\kappa}(r_o)(h^2+r_o^2)}}\Big)f_{R_o}^M(r_o|u,\sigma_M)\,\mathrm{d}r_o\Big)\Big)u\,\mathrm{d}u\Big). \quad (29)$$

References

[1] A. Al-Hourani, S. Kandeepan, and S. Lardner, "Optimal lap altitude for maximum coverage," *Wireless Communications Letters, IEEE*, vol. 3, no. 6, pp. 569–572, 2014.

[2] M. Mozaffari, W. Saad, M. Bennis, and M. Debbah, "Drone small cells in the clouds: Design, deployment and performance analysis," *arXiv preprint arXiv:1509.01655*, 2015.

[3] S. Rohde, M. Putzke, and C. Wietfeld, "Ad hoc self-healing of ofdma networks using uav-based relays," *Ad Hoc Networks*, vol. 11, no. 7, pp. 1893–1906, 2013.

[4] S. Chandrasekharan, K. Gomez, A. Al-Hourani, S. Kandeepan, T. Rasheed, L. Goratti, L. Reynaud, D. Grace, I. Bucaille, T. Wirth, *et al.*, "Designing and implementing future aerial communication networks," *arXiv preprint arXiv:1602.05318*, 2016.

[5] A. M. Hayajneh, S. A. R. Zaidi, D. C. McLernon, and M. Ghogho, "Optimal dimensioning and performance analysis of drone-based wireless communications," in *Globecom Workshops (GC Wkshps)*, pp. 1–6, IEEE, 2016.

[6] A. M. Hayajneh, S. A. R. Zaidi, D. McLernon, and M. Ghogho, "Drone empowered small cellular disaster recovery networks for resilient smart cities," in *2016 First International Workshop on Toward A City-Wide Pervasive EnviRonment (SECON Workshops) (CoWPER'16)*, (London, United Kingdom), June 2016.

[7] M. Mozaffari, W. Saad, M. Bennis, and M. Debbah, "Optimal transport theory for power-efficient deployment of unmanned aerial vehicles," *arXiv preprint arXiv:1602.01532*, 2016.

[8] Y. Zeng and R. Zhang, "Energy-efficient uav communication with trajectory optimization," *IEEE Transactions on Wireless Communications*, vol. 16, no. 6, pp. 3747–3760, 2017.

[9] M. Mozaffari, W. Saad, M. Bennis, and M. Debbah, "Mobile internet of things: Can uavs provide an energy-efficient mobile architecture?," *arXiv preprint arXiv:1607.02766*, 2016.

[10] M. Afshang and H. S. Dhillon, "Poisson cluster process based analysis of hetnets with correlated user and base station locations," *arXiv preprint arXiv:1612.07285*, 2016.

[11] C. Saha, M. Afshang, and H. S. Dhillon, "Poisson cluster process: Bridging the gap between ppp and 3gpp hetnet models," *arXiv preprint arXiv:1702.05706*, 2017.

[12] R. Hernandez-Aquino, S. A. R. Zaidi, M. Ghogho, D. McLernon, and A. Swami, "Stochastic geometric modeling and analysis of non-uniform two-tier networks: A stienens model-based approach," *IEEE Transactions on Wireless Communications*, vol. 16, no. 6, pp. 3476–3491, 2017.

[13] S. Srinivasa and M. Haenggi, "Distance distributions in finite uniformly random networks: Theory and applications," *IEEE Transactions on Vehicular Technology*, vol. 59, no. 2, pp. 940–949, 2010.

[14] S. N. Chiu, D. Stoyan, W. S. Kendall, and J. Mecke, *Stochastic geometry and its applications*. John Wiley & Sons, 2013.

[15] 3GPP, "Digital cellular telecommunications system (phase 2+); radio network planning aspects," tech. rep., 3GPP TR 43.030, 2010.

[16] Z. Khalid and S. Durrani, "Distance distributions in regular polygons," *IEEE Transactions on Vehicular Technology*, vol. 62, no. 5, pp. 2363–2368, 2013.

[17] M. Ahsanullah and V. B. Nevzorov, *Order statistics: examples and exercises*. Nova Publishers, 2005.

[18] Y. S. Soh, T. Q. Quek, M. Kountouris, and H. Shin, "Energy efficient heterogeneous cellular networks," *IEEE Journal on Selected Areas in Communications*, vol. 31, no. 5, pp. 840–850, 2013.